Comparison of direct and indirect performance measurements of an externally wetted, passively fed electrospray thruster

IEPC-2024-737

Presented at the 38th International Electric Propulsion Conference, Toulouse, France
June 23-28, 2024

Borja De Saavedra* and David Villegas-Prados† and Mick Wijnen‡
IENAI SPACE, Leganés, Madrid, 28919, Spain

Pablo Fajardo§
Universidad Carlos III de Madrid, Leganés, Madrid, 28911, Spain

Interest in ionic liquid electrospray propulsion has increased considerably in recent years due to its potential for high specific impulse and efficiency at low power, making it a promising solution for the fast-growing small satellite market. However, electrospray thrusters present the challenge of measuring very low thrust and mass flow rates for performance characterization. Although direct thrust measurements are common practice in the literature, propellant consumption is rarely measured in situ, being typically estimated through mass spectrometry separately. In this work, a modified analytical balance was used in tandem with a time-of-flight mass spectrometer to obtain both direct and indirect thrust and mass flow rate measurements. An electrostatic calibration device built with commercial-off-the-shelf heat sinks was characterized with high-precision calibration weights and then used in vacuum to correct the measurements of the balance. Direct thrust and mass loss rate measurements of the order of μN and mg/h or less, respectively, were acquired consistently at the same time. An average relative difference of 10.5% was found between direct and indirect thrust measurements, with a consistent thrust-to-current ratio of 0.1 μN/μA. On the other hand, the mass flow rate estimated with time-of-flight mass spectrometry was between 23.1% and 64.7% lower than the mass loss rate obtained with the balance. Possible reasons for this disagreement and methods to assess them are discussed.

*Head of Qualification, Diagnostics and Testing, Electric Propulsion Department, borja.desaavedra@ienai.space.
†Propulsion and Design Engineer, Electric Propulsion Department, david.villegas@ienai.space.
‡Chief Technology Officer, Electric Propulsion Department, mick.wijnen@ienai.space.
§Professor, Department of Aerospace Engineering, pfajardo@ing.uc3m.es.

I. Introduction

The unceasing miniaturization of electronics is driving the growth of the small satellite market at an accelerated rate. In 2021, small satellites amounted to 94% of all launched spacecraft and 43% of the total upmass.[1] Although electric propulsion systems are increasingly being incorporated on space missions,[2] conventional (plasma) thrusters are falling behind the surge of microsatellites and nanosatellites. Size reduction of these propulsion systems is complicated and typically results in a significant efficiency decrease.

On the other hand, the interest in electrospray thrusters is increasing due to their small size and their potential for high efficiency at low power. Unlike other propulsion technologies, miniaturization of electrospray devices presents no inherent efficiency loss mechanism.[3] Furthermore, the progress of microfabrication technologies allows for high current density electrospray emitters,[4] with performances similar to ion and Hall thrusters[5] at a lower power.

Electrospray thrusters produce thrust by extracting and accelerated charged particles from a conductive liquid with an applied electric field. A substrate called emitter is wet with the conductive liquid and an electric potential difference is applied between the liquid and an extractor grid. At high electric field strengths, the liquid forms a meniscus and emits ions or charged droplets, which are accelerated by the field and produce thrust.[6] A schematic is shown in Figure 1. Electrospray thrusters can operate in different regimes, depending on the type of emitted particles: the cone-jet regime, in which a jet is formed that breaks up into droplets, the purely ionic regime, in which evaporation of ions occurs directly from the meniscus tip, and the mixed regime, in which both droplets and ions are emitted. The local electric field strength needed for emission is very high, $\sim$ 0.1–1 V/nm for ions.[7] To reduce the required electric potential for operation, emitters feature sharp tips to enhance the field strength. An array of these sharp structures is typically included in electrospray emitters, which are categorized by geometry into capillary,[8] porous[9] or externally wetted.[10]

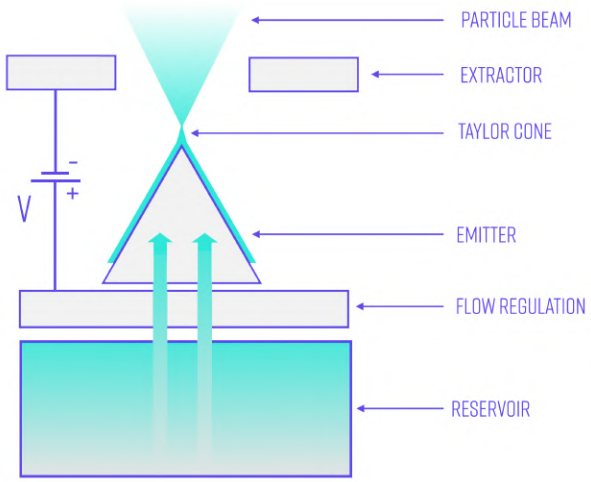

Figure 1: Externally wetted electrospray thruster schematic.

Room temperature ionic liquids (RTILs), which are molten salts that consist of both positive and negative chemically stable molecular ions, are typical propellants used in electrospray thrusters. The main advantages of these liquids are that particles of both polarities can be emitted, thus removing the need of a neutralizer,[11] and their negligible vapour pressure, which is convenient for storage without pressurization. Electrospray thrusters using RTILs typically emit in the purely ionic regime or with some droplet emission (mixed regime), although the choice of liquid can significantly affect the performance.[12]

Experimental electrospray thrusters that operate at very low power render direct performance characterization challenging. In general, $\sim$ 1 μA of emitted current is produced per emitter tip. With a thrust-to-current ratio of the order of $\sim$ 0.05 – 0.1 μN/μA,[9] an array of hundreds of emitter tips typically generates a thrust of a few micronewton. Direct thrust characterization of this order with torsional thrust stands is common practice in the literature.[13,14] Analytical balances are increasingly being used for direct thrust measurements of electrospray thrusters.[15–17] However, to estimate specific impulse and efficiency, the mass

flow rate is also required. The standard practice is to perform time-of-flight mass spectrometry and other indirect diagnostics separately to estimate the overall performance of the thruster. Although some direct mass flow rate measurements (in situ) can be found in the literature,[17,18] it is far from common. Experimental electrospray thrusters typically exhibit a mass flow rate of the order of mg/h or less, which makes direct characterization complex. This requires operating a balance in the vertical direction and ensuring proper calibration since outgassing, environmental drift, and other perturbations can alter considerably the mass loss measurements.

In this work, a modified analytical balance (Mettler Toledo AX504) equipped with an electrostatic calibration device (ECD) was used to characterize the performance of an externally wetted, passively fed electrospray thruster. A dedicated experimental setup was used to arrange a time-of-flight mass spectrometer in tandem with the balance to attain indirect thrust and mass flow rate measurements simultaneously, in order to compare the performance results from the two diagnostics. The experimental thruster was operated with 1-ethyl-3-methylimidazolium bis(trifluoromethylsulfonyl)imide (EMI-Im) as propellant.

II. Experimental setup

1. Balance

The MT-AX504 (Figure 2) is a high-precision analytical balance with a maximum load of 510 g and a readability of 0.1 mg. It is a null balance operating on the principle of electromagnetic force restoration: the load on the weighing plate pushes a lever mechanism, which is monitored with a displacement sensor, and an electromagnetic coil on the other end is actuated through feedback control to balance the lever and bring the displacement to zero.

Figure 2: Mettler Toledo AX504.

An electrostatic calibration device (ECD) based on the concept of a comb-drive was built following the work of Chea et al. using commercial off-the-shelf (COTS) heat sinks, since they were shown to generate consistent forces from a few micronewton to millinewtons with less than 2% deviation error.[19] The ECD comprises two Fischer Elektronik ICK BGA 27x27x22 heat sinks modified to act as electrostatic combs with 5x4 pairs of fingers (Figure 3).

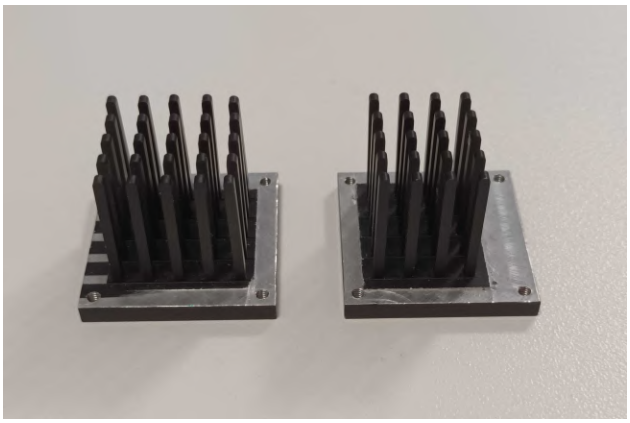

Figure 3: Modified heat sinks used as electrostatic combs for the ECD.

To adapt the balance for operation in vacuum, it was disassembled and all components not strictly necessary were removed. The electronics were separated from the body of the balance, to be kept on the air side. An H-shaped aluminium part with mounting points for other components was added to the fixed part of the balance. The original weighing plate was drilled to incorporate an adaptor plate for the thruster and the mobile part of the ECD to be mounted on. Two 3D printed resin parts were used to hold the electrostatic combs of the ECD, one of them fixed to the front part of the balance, with a safe high voltage (SHV) connector for biasing, and the other one screwed to the adaptor plate, which was electrically connected to ground. The front view of the balance setup, with the ECD and the thruster, is shown in Figure 4.

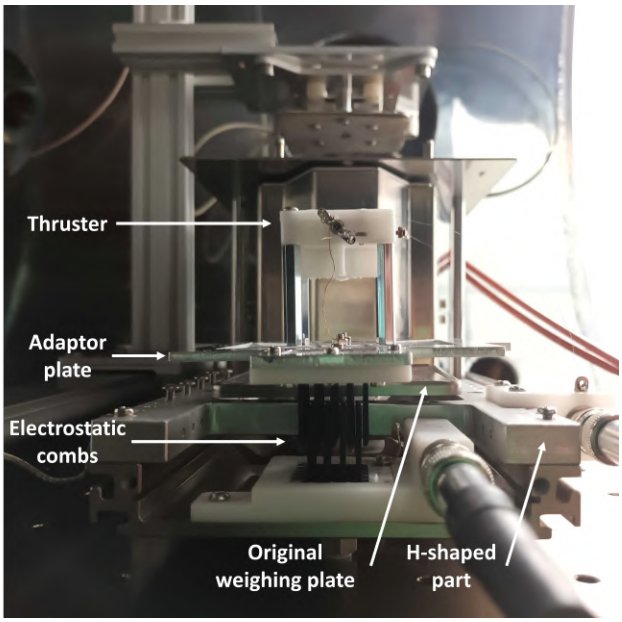

Figure 4: Front view of the balance setup, showing the ECD, the adaptor plate on the mobile part of the balance, and the thruster mounted on hex spacers.

A set of class F1 high-precision calibration weights (standard OIML R 111-1[20]) ranging from 1 mg to 500 g was used to characterize the ECD in atmospheric conditions, correcting for air density and local gravity. Then, the characteristic function of the ECD was used before operating the thruster in order to correct the measurements of the balance in vacuum.

2. Time-of-flight mass spectrometer

The time-of-flight mass spectrometer (ToF) was developed in-house. It is similar to others in the literature[21] and has been used in other published work.[10,12,22] It is composed of an electrostatic deflection gate operated with a high voltage pulse generator, a collector plate at the end of an extension tube, and a secondary electron repeller (SER) – a grid in front of the collector biased negatively (Figure 5). The collector current was measured with a high-speed transimpedance amplifier (TIA) connected to a digital oscilloscope.

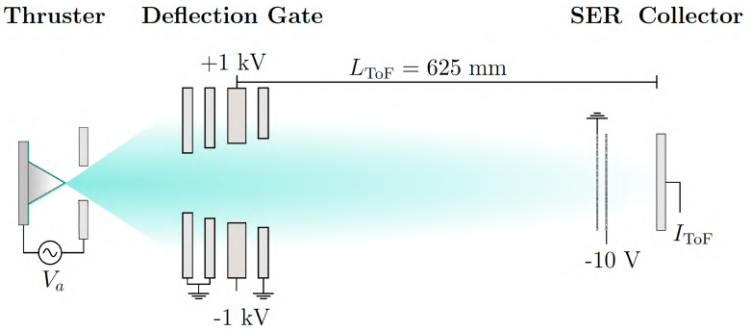

Figure 5: Time-of-flight mass spectrometer schematic. Adapted from Villegas-Prados et al.[10]

The ToF gate, positioned a few centimetres from the thruster extractor, is composed of two plates biased to opposite polarities to produce a perpendicular electric field with respect to the thruster plume, acting as an electrostatic shutter. The high-voltage pulse generator applies ± 1 kV to the electrodes of the gate (2 kV differential voltage) in pulses of 2.5 ms. During these, charged particles emitted by the thruster will be deflected away, and thus only those past the gate, in the so called flight region, will reach the collector. The flight length, L_{ToF}, is the distance between the gate and the collector (625 mm in this setup). A given charged particle of species s will be accelerated to a velocity v_s according to its charge-to-mass ratio $\left(\frac{q}{m}\right)_s$ for a given beam potential ϕ_b, and thus will reach the ToF collector after a time t_s:

$$t_s = \frac{L_{\mathrm{ToF}}}{v_s} = \frac{L_{\mathrm{ToF}}}{\sqrt{2\left(\frac{q}{m}\right)_s \phi_b}} \tag{1}$$

The aggregate of all emitted species produces a current distribution in time at the collector. Ions have defined charge-to-mass ratios according to their degree of solvation n, with chemical formulae: $[\mathrm{EMI\text{-}Im}]_n$ EMI^+ (cation) and $[\mathrm{EMI\text{-}Im}]_n$ Im^- (anion). Table 1 shows the molecular masses of monomers ($n = 0$), dimers ($n = 1$) and trimers ($n = 2$). Ions with higher degrees of solvation were not observed in this work. On the other hand, droplets exhibit a continuous current distribution since they have different sizes and thus a dispersion of charge-to-mass ratio.

Degree of solvation	**Molecular mass (Da)**	
	Cation	**Anion**
$n = 0$	111.2	280.1
$n = 1$	502.5	671.5
$n = 2$	893.8	1062.8

Table 1: Molecular masses of 1-ethyl-3-methylimidazolium bis(trifluoromethylsulfonyl)imide ions with degree of solvation $n \leq 2$.

The ToF gate was mounted on a motorized linear stage to control its position in vacuum, in order to place it in front of the thruster (engaged position) when desired. The collector is an aluminium disk with a diameter of 90 mm and a thickness of 1 mm. The SER was placed 5 mm upstream the collector and is composed of two meshes, 5 mm apart: the one closer to the thruster grounded to the vacuum chamber and the other one biased to -10 V. The high-speed TIA (FEMTO DHCPA-100) was connected to the feedthrough directly to lower the input capacitance, and was used with a gain of 100 kV/A (1.8 MHz bandwidth).

3. Vacuum facility

The vacuum chamber is a 0.8 m diameter, 1 m long cylinder, with an extension tube 100 mm in length and 160 mm in diameter added to a top flange for the ToF collector. The thruster was positioned on the balance, to fire vertically towards the ToF collector. The vacuum facility includes a Leybold SCROLLVAC 10 plus roughing pump and a Leybold TURBOVAC 450 iX turbomolecular pump, with a nominal pumping speed of 450 L/s. A pressure of about $7 \cdot 10^{-5}$ mbar was maintained in the vacuum chamber during thruster operation.

4. Electrospray thruster

An externally wetted, passively fed experimental electrospray thruster was operated with 1-ethyl-3-methylimidazolium bis(tri-fluoromethylsulfonyl)imide (EMI-Im) as propellant. It is composed of a bottom part, a propellant deposit, a fluidic interface, an emitter with a frame, an extractor and a top part (Figure 6).

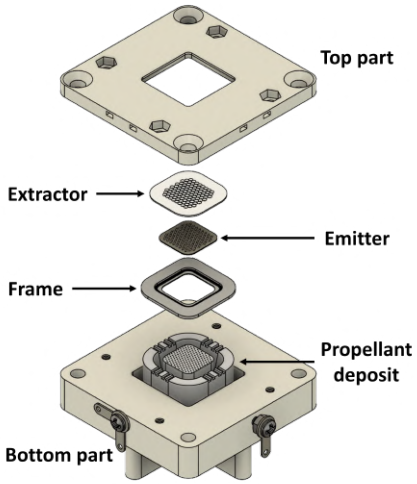

Figure 6: Exploded view of the experimental thruster unit.

The deposit is 3D printed in aluminium and can hold up to 45 μL of propellant in an array of channels 300 μm in diameter. The emitter is made of silicon and comprises an array of 101 tips, with several feeding holes surrounding each of them. Nanostructures cover the entire surface of the emitter in order to drive the ionic liquid by capillarity from the feeding holes to the tips. A nylon filter acts as fluidic interface between the back of the emitter and the propellant deposit. The extractor grid is made of borosilicate glass, with an aluminium coating on top.

The channels in the propellant deposit wick up the ionic liquid, wetting the nylon filter on contact. Then, capillary forces drive the liquid through the emitter feeding holes, and between the nanostructures up to the tips of the cones. A distal electrode approach was followed to mitigate electrochemical reactions at the emitter tips[23] by making the high voltage connection at the propellant deposit. The extractor electrode was grounded to the vacuum chamber. The connections were made with 0.1 mm diameter silver-plated copper wire filaments soldered from ring terminals on the thruster to an SHV connector on the fixed part of the balance. The reduced thickness of the filaments and the strain relief provided by the connector prevent the thruster connections from disturbing the balance measurements.

The thruster was fired at all emitter voltages between 1300 V and 2000 V in steps of 100 V for about 30 minutes each. An automatic current compensation algorithm was used to prevent charge buildup in the ionic liquid since the emitted current is larger in the positive polarity. A trapezoidal signal as shown in Figure 7 was used to operate the thruster, starting with the negative polarity. The nominal voltages were set to the emitter voltage in each case: $V_1 = -V_e$, $V_2 = V_e$. The nominal negative time and the ramp time used are $t_1 = 1$ s and $t_r = 0.1$ s, respectively. The nominal positive time t_2 was determined in every cycle

by the compensation algorithm according to:

$$\int_0^{t_1+2t_r} I_e dt = \int_{t_1+2t_r}^{t_1+t_2+3t_r} I_e dt \tag{2}$$

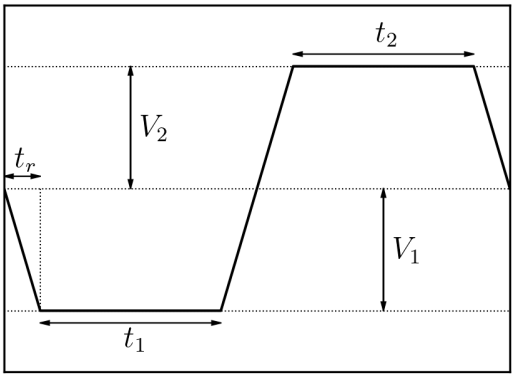

Figure 7: Emitter voltage trapezoidal signal.

In order to obtain reliable direct mass loss rate measurements, a linear drift correction approach[17,18] was followed to correct for environmental drift and possible outgassing. The balance was operated before and after each thruster firing for 30 minutes while keeping the thruster off. The background force drift was obtained from the average of the linear regression of the force in these periods, and then subtracted from the measurements during the firings to compute the mass loss rate of the thruster.

Before closing the vacuum chamber, the balance was positioned to align the ToF gate in the engaged position with the axis of the thruster. An image of the experimental setup is shown in Figure 8. The ToF gate was engaged (in front of the thruster exhaust) during all firings. ToF measurements were obtained periodically in batches of 800 curves, acquiring 7 batches at each emitter voltage.

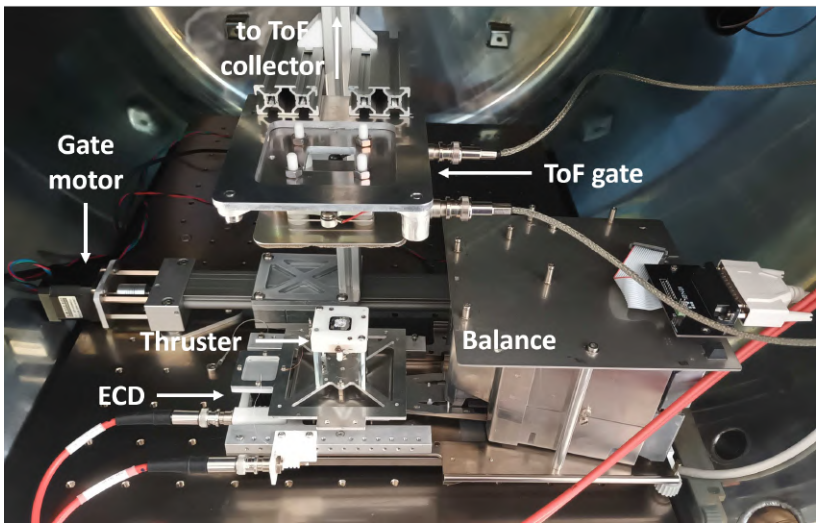

Figure 8: Full experimental setup, with the electrospray thruster mounted on the balance and its axis aligned with the ToF gate (engaged).

III. Results

The temperature measured by the balance ranged between 20.4°C and 21.0°C. The balance showed high stability, with linear force drifts of few μN/h before and after the thruster firings. The average linear drift

regression values for each firing are shown in Table 2 in chronological order. The drift before and after the firing at 1700 V is shown in Figure 9 as a representative case.

Firing	1	2	3	4	5	6	7	8
Emitter voltage (V)	1800	1700	1600	1500	1400	1900	1300	2000
Force drift (μN/h)	-6.9	-1.9	+1.4	+1.8	+1.7	+1.2	-5.1	-4.3

Table 2: Average balance force drift for each thruster firing.

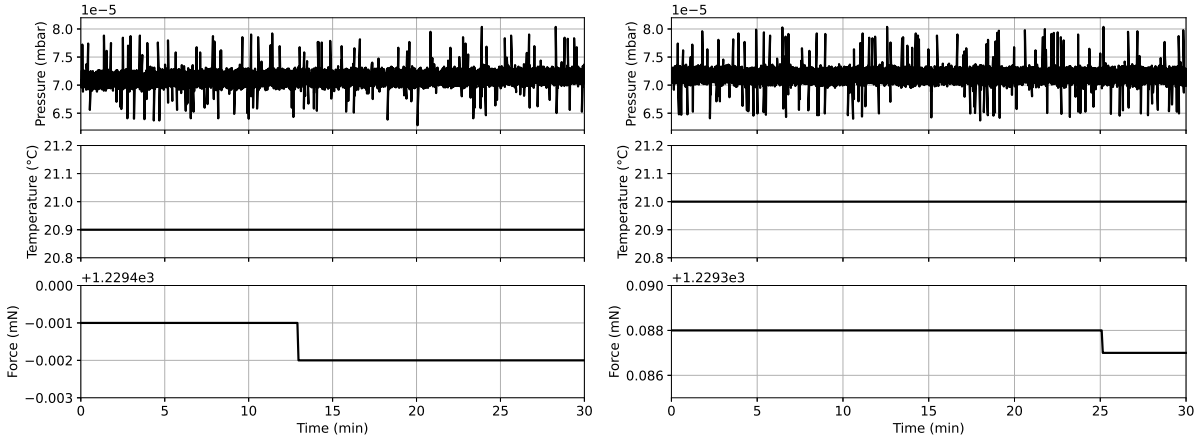

(a) Before firing. (b) After firing.

Figure 9: Pressure, temperature and force during balance drift measurement periods before and after the thruster firing at 1700 V.

The force measured by the balance showed a linear decrease in time during the firings, including both the background force drift and the mass loss rate corresponding to propellant extraction. The emitter voltage, emitted current and raw force measurements during a representative firing (1700 V) are shown in Figure 10.

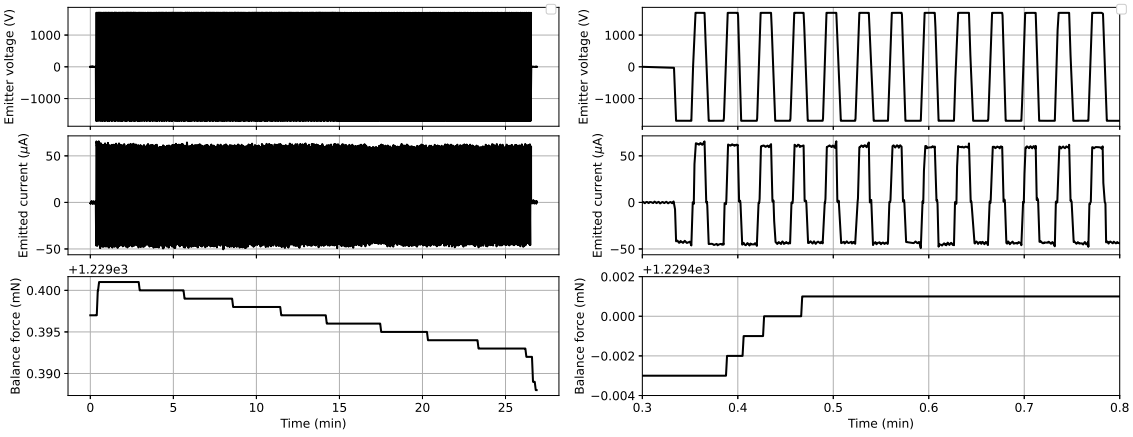

(a) (b)

Figure 10: Emitter voltage, emitted current and raw force measurements during thruster firing at 1700 V: (a) entire firing, (b) close-up of firing start.

The emitted current was very stable in all firings. A linear dependence on emitter voltage was found with a regression slope of 0.078 ± 0.004 μA/V (Figure 11). This is consistent with the emission of similar emitters at a voltage sufficiently above onset.[10] The automatic current compensation algorithm resulted in unequal

nominal times per polarity given the difference in positive and negative emitted current. The positive and negative duty cycles ranged between 24.9% – 30.9% and 44.4% – 48.4%, respectively.

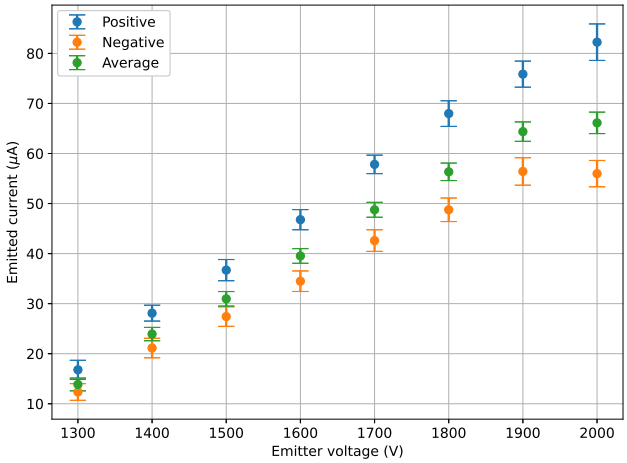

Figure 11: Positive, negative and average nominal emitted current against emitter voltage for all firings.

The results of the time-of-flight mass spectrometry showed little difference during the firings, which is consistent with the observed emission stability. Representative ToF curves for positive and negative emission are shown in Figure 12, which correspond to the average curve of the batch at the midpoint of the firings at 1300 V, 1500 V, 1700 V and 1900 V.

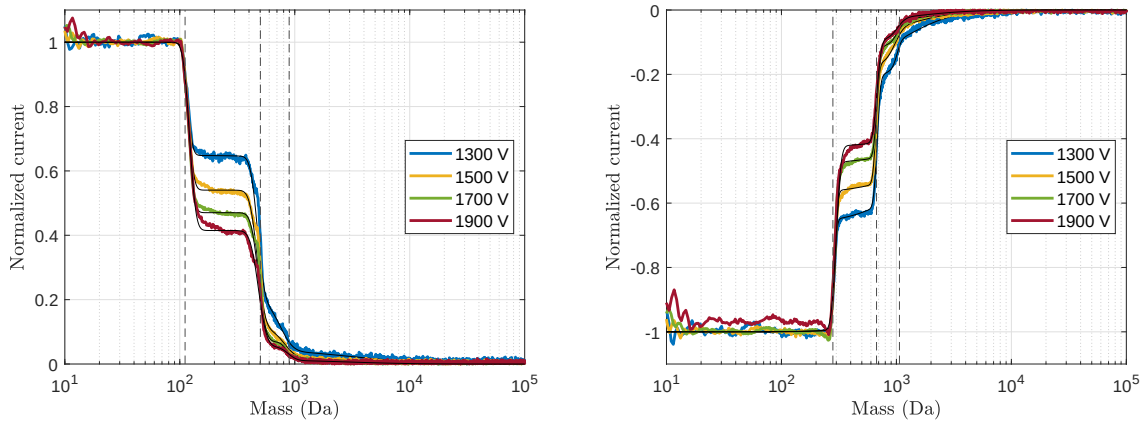

(a) Positive emission.

(b) Negative emission.

Figure 12: Average time-of-flight mass spectrometry curves at the midpoint of thruster firings at different emitter voltages for positive (a) and negative (b) emission. Black continuous lines are the curve fittings. Vertical dashed lines are shown to highlight the molecular masses of monomers, dimers and trimers.

Direct and indirect performance parameters are gathered in Figure 13 for all thruster firings. Thrust agrees within -9.3% – +15.0% relative difference between the two methods for most cases, except at 1300 V, 1400 V (close to the resolution of the balance) and at 2000 V, where the direct thrust is apparently an outlier. Thrust linearity with emitted current is observed consistently, with an average ratio of 0.104 ± 0.002 μN/μA, and 0.108 ± 0.019 μN/μA for indirect, direct results, respectively. The thrust-to-power ratio concurs accordingly, ranging between 50 and 70 μN/W.

On the other hand, a considerable discrepancy in mass flow rate was found between direct and indirect, the latter being between 23.1% and 64.7% lower. Consequently, the specific impulse from direct measurements ranges between 500 s and 1500 s, whereas the indirect characterization yields 1500 s – 2300 s. An increasing trend with emitter voltage is observed in both methods.

The thrust efficiency obtained from direct measurements is seen to increase with emitter voltage from 10% to about 28% at 1900 V. The notably larger thrust observed at 2000 V, which seems to be an outlier, causes the efficiency to rise to 56.8%. In opposition, the indirect thrust efficiency decreases slightly with emitter voltage, from around 62% to 59%.

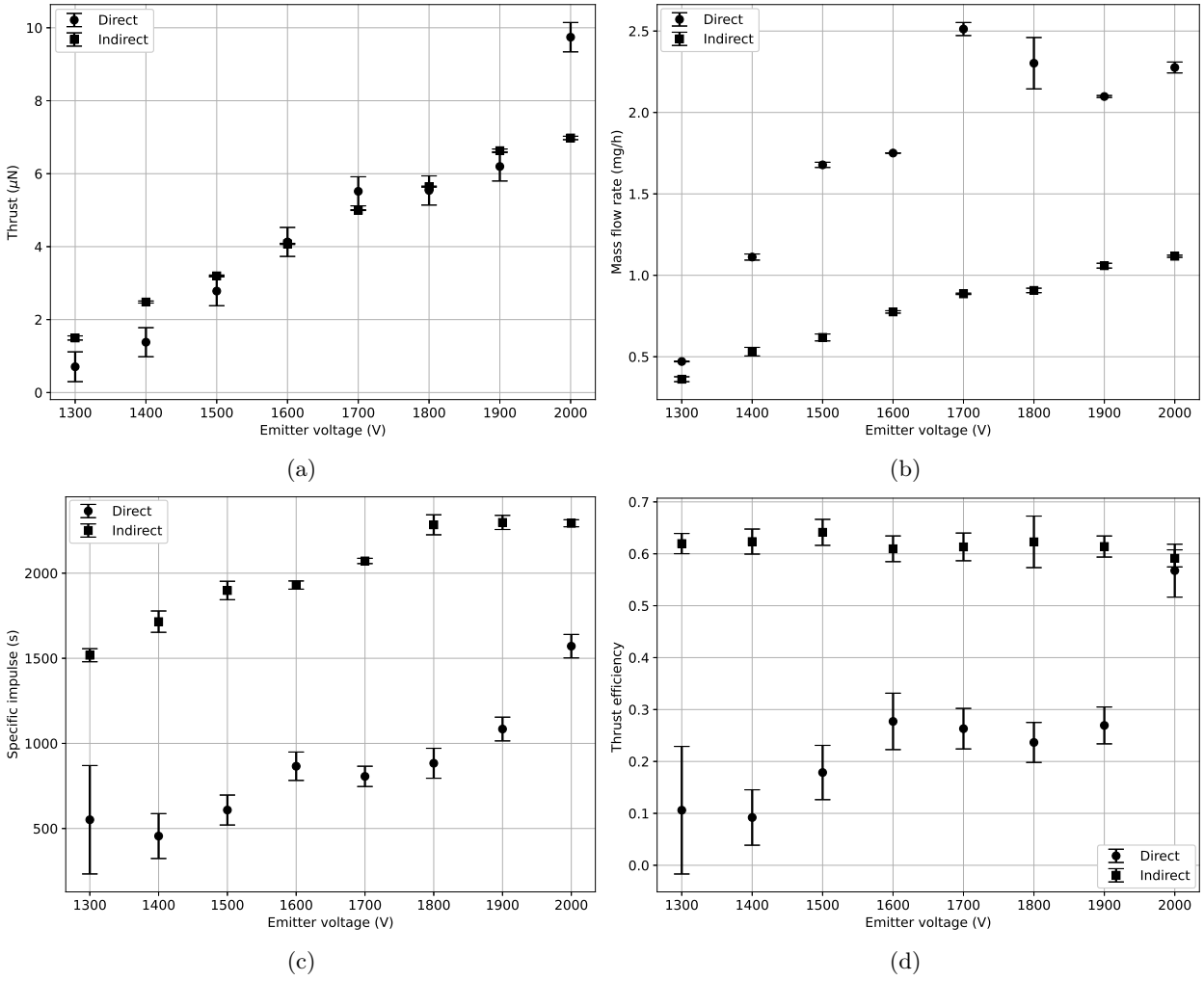

Figure 13: Thruster performance results: (a) thrust, (b) mass flow rate, (c) specific impulse, (d) thrust efficiency.

IV. Discussion on performance results

Despite the discrepancy in mass flow rate results, the concordance of thrust between direct and indirect methods confirms the validity of the ToF measurements, given that both parameters are computed from the same current distribution. Thrust was confirmed to be dominated by the emitted current, which agrees with the thrust equation

$$F_T = I_e \sqrt{2V_e \langle \frac{m}{q} \rangle \eta_T}, \tag{3}$$

since the mass-to-charge ratio decreases with emitter voltage while the efficiency rises, so their product under the square root does not vary significantly. As a matter of fact, the thrust-to-emitted-current ratio was observed to be constant, ≈ 0.1 μN/μA, in all cases.

Three main reasons for the disagreement between direct and indirect mass flow rates were identified. In the first place, emission during the voltage ramps. Time-of-flight measurements were taken during the

flat parts of the trapezoidal voltage signal (nominal conditions), whereas balance measurements are time-averaged, i.e. they include the entire cycle of the signal. Although the nominal duty cycle was used to correct the direct measurements, the emission during the ramps was neglected, which amounts to about one quarter of the period. Considering that the onset voltage was about 900 V, the thruster would be emitting for an additional 8.2% – 14.0% (1300 V – 2000 V) of the cycle, which was unaccounted for. This would contribute to the discrepancy between balance and time-of-flight results, especially for mass flow rate since the droplet fraction increases at lower voltages. As shown in Figure 12, droplets present a mass-to-charge ratio spanning over $\sim 10 - 100$ mg/C ($10^3 - 10^4$ Da per elementary charge), and their current fraction is reduced with emitter voltage. Monomers and dimers carry most of the current ($> 90\%$), with an average molecular mass of ~ 390 Da. Therefore, only a few percent of droplet current could represent more than half of the total emitted mass, given the $\sim 3 - 25$ times larger mass-to-charge ratio of droplets.

In addition, it is theorized that a layer of ionic liquid can be accumulated in the time below onset, and be expelled during the voltage transient, producing more droplets than in the steady-state emission. Current surges have been observed for fast voltage transients in externally wetted electrospray emitters,[24] although the ramps used here are much slower.

A second phenomenon contributing to the mass flow rate discrepancy could be off-axis emission. The presence of multiple emission sites has been reported for porous electrospray emitters,[25] showing an increasing number of sites per tip with emitter voltage. Although the thruster used in this work is not porous but externally wetted, the nanostructures on the surface of the emitter tips serve as anchor points for the ionic liquid, potentially forming several menisci on the same emitter tip. Indeed, off-axis emission was detected in previous experimental thrusters. The beam divergence observed with Angular Faraday probe measurements would imply no impact on the extractor considering the geometry of the thruster. However, intercepted current was measured at the extractor. This would be justified by additional, off-center emission sites, generating secondary beams at a large angle with respect to the axis of the tips. This could considerably increase the mass flow rate while not contributing significantly to thrust. Furthermore, the electric field strength at these off-center sites would be lower, their beams hence containing a larger droplet fraction. Since the time-of-flight mass spectrometer captures only a small portion of the beam, this would be consistent with the mass flow rate disagreement while having similar thrust.

A third mechanism potentially contributing is neutral mass loss during thruster operation through decomposition of the ionic liquid. Electrochemical reactions can occur between the ionic liquid and the high voltage electrode,[26] causing it to break down into other organic compounds. The cation of the ionic liquid used in this work, EMI^+, is well known to be electrochemically unstable due to its proton on the C2 position on the imidazolium ring.[27] This can trigger a series of reactions, potentially resulting in several neutral volatile products, depending on the exact decomposition pathway. In addition, back-streaming of high-velocity particles or arcing can raise locally the temperature of the liquid, potentially causing thermal decomposition[14] and thus further neutral mass evaporation. Whereas the ToF would not capture this neutral mass loss rate, the measurements of the balance would include it.

V. Conclusion

The modification of the analytical balance and the addition of the electrostatic calibration device permitted high-precision direct thrust and mass loss rate measurements, with maximum propagated uncertainties of 0.4 μN and 0.16 mg/h, respectively. Furthermore, thanks to the novel experimental setup, the time-of-flight mass spectrometer could be operated in tandem with the balance, attaining indirect measurements simultaneously.

Thrust results showed less than 15% relative difference between the direct and indirect diagnostics in most cases. Thrust was mostly dependent on the emitted current, exhibiting a constant ratio of ≈ 0.1 μN/μA. On the other hand, a considerable difference was found in mass flow rate, the indirect results being lower in all cases (between 23.1% and 64.7%). This could not be justified by the propagated uncertainty, even including the maximum difference in background force drift.

The mass flow rate discrepancy brings about ambiguity regarding the actual propellant consumption of the thruster. The significance of this disagreement in terms of specific impulse and efficiency depends on the actual reason behind it.

The emission during the voltage ramps being unaccounted for is certain. Time-of-flight measurements

thus underestimate the overall mass flow rate, but the actual extent of this depends on the emission dynamics during the transients, which remain unknown. To assess this, ToF measurements could be taken selectively in time, including during the voltage ramps.

Off-axis emission at a large angle on account of multiple emission sites would also render the indirect results inaccurate. To evaluate this phenomenon, time-of-flight measurements could be performed at different angles with respect to the axis of the thruster plume.

Neutral mass evaporation would only affect the measurements of the balance, the direct method hence overestimating the actual *ionized* mass flow rate. The neutral mass would be lost without contributing to thrust, which would entail an ionization efficiency lower than unity. To avoid this, breakdown of the ionic liquid could be mitigated. To prevent electrochemical reactions, a larger interface area between the high voltage electrode and the ionic liquid would increase the emitted charge required to exceed the electrochemical window of the liquid.[26] In turn, longer nominal times could be used, which would also reduce the aforementioned contribution of voltage transients. On the other hand, kinetic decomposition of the ionic liquid would be caused by back-streaming particles. A larger vacuum chamber or specific beam targets could help, but it can always occur to some extent.

The modification of an analytical balance for operation in vacuum is presented as a cost-effective, high-precision solution for direct thrust and propellant consumption measurements. To the best of the authors' knowledge, it is the first time full direct performance characterization has been reported for an externally wetted electrospray thruster, and the first time direct thrust measurements have been acquired simultaneously with time-of-flight mass spectrometry for an electrospray thruster of any type. This has permitted identifying possible mass loss mechanisms that would otherwise go unnoticed when relying only on the mass spectrometer. The propellant consumption discrepancy will be investigated further in future work.

Acknowledgments

This work was supported by the Spanish Ministry of Science and Innovation (MICINN), under the program "Ayudas para contratos para la formación de doctores en empresas (Doctorados Industriales) 2019", with reference DIN2019-010623.

References

[1]Bryce Tech, Smallsats by the Numbers, https://brycetech.com/reports/report-documents/Bryce_Smallsats_2022.pdf (2022).

[2]D. Lev, R. M. Myers, K. M. Lemmer, J. Kolbeck, H. Koizumi, K. Polzin, The technological and commercial expansion of electric propulsion, Acta Astronautica 159 (2019) 213–227. doi:https://doi.org/10.1016/j.actaastro.2019.03.058.

[3]D. Krejci, P. Lozano, Space propulsion technology for small spacecraft, Proceedings of the IEEE 106 (3) (2018) 362–378. doi:10.1109/JPROC.2017.2778747.

[4]T. Henning, K. Huhn, L. W. Isberner, P. J. Klar, Miniaturized electrospray thrusters, IEEE Transactions on Plasma Science 46 (2) (2018) 214–218. doi:10.1109/TPS.2017.2755373.

[5]A. R. Tummala, A. Dutta, An overview of cube-satellite propulsion technologies and trends, Aerospace 4 (4) (2017). doi:10.3390/aerospace4040058.

[6]M. Gamero-Castano, V. Hruby, Electrospray as a source of nanoparticles for efficient colloid thrusters, Journal of Propulsion and Power 17 (5) (2001) 977–987. doi:10.2514/2.5858.

[7]C. Coffman, M. Martínez-Sánchez, F. J. Higuera, P. C. Lozano, Structure of the menisci of leaky dielectric liquids during electrically-assisted evaporation of ions, Applied Physics Letters 109 (23) (2016) 231602. doi:10.1063/1.4971778.

[8]S. Dandavino, C. Ataman, C. N. Ryan, S. Chakraborty, D. Courtney, J. P. W. Stark, H. Shea, Microfabricated electrospray emitter arrays with integrated extractor and accelerator electrodes for the propulsion of small spacecraft, Journal of Micromechanics and Microengineering 24 (7) (2014) 075011. doi:10.1088/0960-1317/24/7/075011.

[9]R. S. Legge, P. C. Lozano, Electrospray propulsion based on emitters microfabricated in porous metals, Journal of Propulsion and Power 27 (2) (2011) 485–495. doi:10.2514/1.50037.

[10]D. Villegas-Prados, J. Cruz, M. Wijnen, S. Correyero, P. Fajardo, J. Navarro-Cavallé, Impact of propellant temperature on the emission regime of an externally wetted electrospray systemusing time-of-flight mass spectrometry, Acta Astronautica 213 (2023) 145–155. doi:https://doi.org/10.1016/j.actaastro.2023.08.045.

[11]P. Lozano, M. Martinez-Sanchez, Efficiency Estimation of EMI-BF4 Ionic Liquid Electrospray Thrusters, 2005. doi:10.2514/6.2005-4388.

[12]D. Villegas-Prados, J. Cruz, M. Wijnen, P. Fajardo, J. Navarro-Cavallé, Emission and performance characterization of ionic liquids for an externally wetted electrospray thruster, Acta Astronautica 219 (2024) 97–107. doi:https://doi.org/10.1016/j.actaastro.2024.03.013.

[13]D. Krejci, F. Mier-Hicks, R. Thomas, T. Haag, P. Lozano, Emission characteristics of passively fed electrospray microthrusters with propellant reservoirs, Journal of Spacecraft and Rockets 54 (2017) 1–12. doi:10.2514/1.A33531.

[14]M. R. Natisin, H. L. Zamora, Performance of a Fully Conventionally Machined Liquid-Ion Electrospray Thruster Operated in PIR, in: 36th International Electric Propulsion Conference (IEPC), Electric Rocket Propulsion Society, 2019.

[15]D. Courtney, S. Dandavino, H. Shea, Comparing direct and indirect thrust measurements from passively fed and highly ionic electrospray thrusters, Journal of Propulsion and Power 32 (2015) 392–407. doi:10.2514/1.B35836.

[16]N. R. Demmons, Z. Wood, N. Alvarez, Characterization of a High Thrust, Pressure-Fed Electrospray Thruster for Precision Attitude Control Applications. doi:10.2514/6.2019-3817.

[17]C. Huang, J. Li, M. Li, Performance measurement and evaluation of an ionic liquid electrospray thruster, Chinese Journal of Aeronautics 36 (3) (2023) 1–15. doi:https://doi.org/10.1016/j.cja.2021.10.030.

[18]M. R. Gilpin, W. A. McGehee, N. I. Arnold, M. R. Natisin, Z. A. Holley, Dual-axis thrust stand for the direct characterization of electrospray performance, Review of Scientific Instruments 93 (6) (06 2022). doi:10.1063/5.0087716.

[19]K. H. Cheah, K.-S. Low, Q.-V. Tran, Z. Lau, Development of an electrostatic calibration system for a torsional micronewton thrust stand, IEEE Transactions on Instrumentation and Measurement 64 (12) (2015) 3467–3475. doi:10.1109/TIM.2015.2476237.

[20]OIML, International Recommendation OIML R 111-1 Edition 2004 (E), International Organization of Legal Metrology, 2004.
URL https://www.oiml.org/en/files/pdf_r/r111-1-e04.pdf

[21]P. C. Lozano, Energy properties of an EMI-Im ionic liquid ion source, Journal of Physics D: Applied Physics 39 (1) (2005) 126. doi:10.1088/0022-3727/39/1/020.

[22]D. Villegas-Prados, M. Wijnen, S. Correyero, G. Arboleya, P. Fajardo, Impact of the propellant temperature on the performance of externally wetted electrospray thrusters, in: 37th International Electric Propulsion Conference (IEPC), Electric Rocket Propulsion Society, 2022.

[23]N. Brikner, P. C. Lozano, The role of upstream distal electrodes in mitigating electrochemical degradation of ionic liquid ion sources, Applied Physics Letters 101 (19) (2012) 193504. doi:10.1063/1.4766293.

[24]P. C. Lozano, M. Martínez-Sánchez, On the dynamic response of externally wetted ionic liquid ion sources, Journal of Physics D: Applied Physics 38 (14) (2005) 2371. doi:10.1088/0022-3727/38/14/011.

[25]R. A. Dressler, B. St. Peter, Y.-H. Chiu, T. Fedkiw, Multiple emission sites on porous glass electrospray propulsion emitters using dielectric propellants, Journal of Propulsion and Power 38 (5) (2022) 809–821. doi:10.2514/1.B38453.

[26]P. Lozano, M. Martínez-Sánchez, Ionic liquid ion sources: suppression of electrochemical reactions using voltage alternation, Journal of Colloid and Interface Science 280 (1) (2004) 149–154. doi:https://doi.org/10.1016/j.jcis.2004.07.037.

[27]K. C. Lethesh, A. Bahaa, M. Abdullah, M. O. Bamgbopa, R. A. Susantyoko, Temperature-dependent electrochemical stability window of bis(trifluoromethanesulfonyl)imide and bis(fluorosulfonyl)imide anion based ionic liquids, Frontiers in Chemistry 10 (2022). doi:10.3389/fchem.2022.859304.